OPEN ACCESS

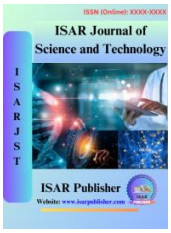

ISAR Journal of Science and Technology
Abbriviate Title- ISAR J Sci Tech
ISSN *(Online)*- 2584-2056
https://isarpublisher.com/journal/isarjst
Vol-2, Iss-6 (June- 2024)

OPEN ACCESS

On dissipative non-slip hydromagnetic flow of Arrhenius kinetics fluid reaction with variable properties

K. O. Ogboru[1], W. A. Adeyemi[2], A. M. Okedoye[3*]

Department of Mathematics, Federal University of Petroleum Resources, Effurun, Nigeria.

***Corresponding Author**

A. M. Okedoye

Department of Mathematics, Federal University of Petroleum Resources, Effurun, Nigeria.

Article History

Received: 07.05.2024
Accepted: 02.06.2024
Published: 11.06.2024

Abstract: The emphasis of this investigation is to examine the non-slip hydromagnetic laminar dissipation flow of Arrhenius kinetics fluid, binary mixture with variable properties and reaction order in a boundless porous vertical device. Without fluid material deformation, the fluid chemical reaction is stimulated by activation energy, branched reaction order and internal heating. The two-dimensional partial derivatives model is transformed into a physical dimensionless thermo-fluid form. With appropriate similarity quantities, the coupled quasi-linear invariant ordinary derivative equations are obtained. Numerical solutions of the invariant dimensionless differential equations are established in tabular and graphical form to demonstrate the sensitivity of entrenched parameters. The investigation outcomes depicted that binary reaction decreased the flow velocity, but raised the chemical reaction species. The material coefficient and activation energy enhanced the heat distribution in the flow medium. Hence, the study will help in industrial development for appropriate selection of their working fluid.

Keywords: Viscous dissipation; Arrhenius kinetics; Reaction order; Activation energy; Non-slip condition Dissipative flow, Hydromagnetic flow, Variable properties, Heat and mass transfer.

Cite this article:

Ogboru, K. O., Adeyemi, W. A., Okedoye, A. M.., (2024). On dissipative non-slip hydromagnetic flow of Arrhenius kinetics fluid reaction with variable properties. *ISAR Journal of Science and Technology*, *2*(6), 1-12.

1. Introduction

The study of fluid dynamics, particularly in the context of hydromagnetic flows, is a critical area of research due to its numerous industrial and engineering applications. Hydromagnetic, or magnetohydrodynamic (MHD), flow concerns the behaviour of electrically conducting fluids in the presence of magnetic fields, which is pertinent in areas such as nuclear reactors, geothermal energy extraction, and electronic cooling systems. The dynamics of such flows become even more complex and interesting when considering reactive fluids governed by Arrhenius kinetics, especially under conditions where fluid properties like viscosity and thermal conductivity are variable. This research aims to investigate the dissipative non-slip hydromagnetic flow of a reactive fluid following Arrhenius kinetics with variable fluid properties. The interactions between the magnetic field, variable fluid properties, and chemical reaction rates poses significant challenges but also offers valuable insights into optimizing industrial processes and enhancing energy efficiency.

In 1904, when Prandtl proposed his assumptions that when viscous fluid flow past a surface, the vicious effects is dominant in a thin layer call the boundary layer, the flow may be regarded as that of an ideal fluid. The boundary layer theory has tremendous achievement to its credit and transformed fluid dynamics into a discipline of great science and engineering importance.

Numerous studies have explored various aspects of MHD flows, Arrhenius kinetics, and variable fluid properties, but integrating these components into a cohesive model remains a challenging task. The following review highlights key contributions and gaps in the literature. Recent studies have expanded on the fundamentals of MHD flows, elucidating the impact of magnetic fields on fluid motion, particularly in electrically conducting fluids. For instance, research by Vishnampet and Anilkumar (2021) explored the effects of MHD on convective heat transfer in nanofluids, highlighting new applications in modern engineering.

Furthermore, Ghosh et al. (2020) provided comprehensive analyses of MHD flows with various boundary conditions, advancing our understanding of MHD dynamics in complex systems. Magnetohydrodynamic (MHD) is the science which deals with the motion of highly conducting fluid in the presence of a magnetic field. The motion of the conducting fluid across the magnetic field generates electric currents which change the magnetic field, and the action of the magnetic field gives rise to mechanical forces which modify the flow of the fluid, Prashant (2017). MHD over a moving plate has various applications in solar structure, astrophysics, geophysics, radio propagation, ionoshpere, interstellar matter and many more. Convective flows of transient oscilatory fluid assume a critical role in aerospace technology,

***Corresponding Author:** A. M. Okedoye

turbo machinery and chemical engineering; such flows emerge because of unsteady boundary, Okedoye et al. (2021).

Ahmed et al. (2015) investigated the exact solution regarding convective heat transfer of a magnetohydrodynamic (MHD) in prensence of Jeffery fluid over a stretching surface. The effect of Joule and vicious dissipation, internal heat source/sink and thermal radiation on the heat transfer characteristics are taken in to account in the presence of a transverse magnetic field. B. Zigta (2018) investigated the effect of thermal radiation, chemical reaction and viscous dissipation on a MHD flow. From the findings, it was discovered among other findings that an increment in both the chemical reaction parameter and molecular diffusivity result in a decrease in concentration.

Nomenclature

u, v	Velocities in respective x and y axes	**Greek Letters**	
k	Uniform thermal conductivity	ϕ	Dimensionless liquid chemical reaction
C	Fluid chemical species	β_c	Species expansion coefficient
R	Reynolds number	γ	Reactivity parameter
C_∞	Concentration of the far stream	λ	Binary chemical reaction parameter
H	Hartmann number	α_1	space heat generation
c_p	Specific heat at constant pressure	ϵ	Positive number $(0 < \epsilon \ll 1)$
T_w	Boundary wall surface heat	w	Condition on the wall
R_G	Universal gas constant	**Dimensionless Group**	
r	Positive integer	N	Buoyancy ratio
Gr	Mass solutal buoyancy parameter	V	Limiting velocity
Fs	Darcy Forchiemann Parameter	Pr	Prandtl number
Sc	Schmidt number	θ	Dimensionless liquid temperature
K_T	Variable thermal conductivity	β	Material constants coefficient
D	Species diffusion	β_τ	Heat expansion coefficient
U	Velocity of the far steam	χ	Generative/destructive reaction parameter
T_∞	Free stream temperature	α_o	heat generation/absorption
T	Fluid temperature	τ	Arrhenius number
C_w	Boundary wall chemical reaction	**Subscripts**	
Ea	Activition energy	∞	Ambient condition
g	Gravitational acceleration		

In the work of Okedoye and Salawu (2018), the solution of unsteady oscillatory MHD boundary layer flow past a moving plate with mass transfer and binary chemical reaction was obtained using perturbation method. The work of Singh (2012) reported on the effect of viscous dissipation on MHD boundary layer flow in a porous medium past a moving vertical plate with suction.

The integration of Arrhenius kinetics into reactive flow models has been extensively studied. Recent works have focused on specific applications such as combustion and polymerization processes. For example, Singh et al. (2023) examined the influence of Arrhenius kinetics on the thermal degradation of polymers, providing crucial insights into reaction mechanisms at elevated temperatures . Additionally, Zhang and Wang (2022) analyzed the impact of temperature-dependent reaction rates in catalytic combustion, enhancing predictive capabilities for industrial applications. Research on variable fluid properties has demonstrated that temperature-dependent viscosity and thermal conductivity can significantly alter flow and heat transfer characteristics. Recent studies, such as those by Das and Jana (2022), have focused on the impact of variable viscosity on boundary-layer flows, leading to more accurate models for engineering applications. Moreover, Kumar et al. (2021) investigated the effects of temperature-dependent thermal conductivity in nanofluids, providing valuable data for optimizing heat transfer systems.

Integrating MHD effects with reactive flows and variable properties has been addressed in a few notable studies. Raptis and Perdikis (2020) investigated the MHD flow of a viscous fluid over a stretching sheet, considering thermal radiation and variable viscosity, and highlighted the

interplay between magnetic fields and variable fluid properties . Similarly, Chamkha and Rashidi (2022) examined unsteady MHD convective heat and mass transfer in the presence of chemical reactions and variable properties, providing new insights into the complex interactions in such systems .

In many practical scenarios, fluid properties such as viscosity and thermal conductivity are not constant but vary with temperature, concentration, or other factors. This variability can significantly affect the flow and heat transfer characteristics of the fluid. Incorporating these variable properties into mathematical models makes the analysis more realistic and applicable to real-world situations. Dissipative flows account for the internal friction within the fluid, which converts kinetic energy into thermal energy, impacting the thermal and velocity fields. The non-slip condition, where the fluid velocity at a solid boundary is zero, is a standard boundary condition in fluid dynamics. This condition, combined with dissipation effects, plays a crucial role in determining the overall behavior of the flow.

From the proceeding investigations, it is observed that the variation of viscousity with temperature and viscous dissipation have diverse application in science and engineering. Hence, we have considered a steady MHD boundary layer flow past a moving vertical plate by taking into consideration the following viscous dissipation.

2. Problem Formulation

A theoretical non-slip hydromagnetic laminar flow of chemical reacting fluid in a vertical boundless device is considered. The flow is influenced by viscous dissipation, varying heat source, pressure gradient and thermal conductivity of temperature dependent without reacting material species consumption. The fluid particles collided continuously without deformation and its satisfied Newton's law of flow motion. The fluid chemical reaction is stimulated by branched reaction order, activation energy, internal heating and chemical kinetics. At low Reynolds number, the magnetic field controls the fluid conductivity strength with negligible magnetic induction. The boundary layer flow equations are formulated based of the highlighted assumptions and it follows from the recent works of [Olarewaju (2021), Okedoye and Salawu (2018)]. Hence, the velocity component, energy and mass equations, as well as the boundary conditions governing the flow are given as:

$$u\frac{\partial u}{\partial x}+ v\frac{\partial u}{\partial y}= -\frac{1}{\rho}\frac{\partial p}{\partial x} + \nu\left[\frac{\partial^2 u}{\partial x^2} + \frac{\partial^2 u}{\partial y^2}\right]-\frac{\sigma\mu B^2(x)}{\rho}(u-U) \mp g\left(\frac{K_1}{\nu}\right)|\hat{u}|(u-U) + g\big(\beta_\tau(T-T_\infty)+\beta_c(C-C_\infty)\big), \tag{1}$$

$$u\frac{\partial v}{\partial x}+ v\frac{\partial v}{\partial y}= -\frac{1}{\rho}\frac{\partial p}{\partial y} + \nu\left[\frac{\partial^2 v}{\partial x^2} + \frac{\partial^2 v}{\partial y^2}\right]-\frac{\sigma\mu B^2(x)}{\rho}v, \tag{2}$$

$$\rho c_p\left(u\frac{\partial T}{\partial x}+ v\frac{\partial T}{\partial y}\right)=\frac{\partial}{\partial y}\left(k\frac{T}{T_\infty}\frac{\partial T}{\partial y}\right)+ \mu\left(\frac{\partial u}{\partial y}\right)^2 -\left(\frac{\kappa u_w(x)}{x\nu}\right)\left[\frac{A^*(T_w-T_\infty)}{bx}(u-U)+B^*(T-T_\infty)\right], \tag{3}$$

$$\rho\left(u\frac{\partial C}{\partial x}+ v\frac{\partial C}{\partial y}\right)=D\frac{\partial^2 C}{\partial y^2}+\gamma(C-C_\infty)-k_r^2(T\ -\ T\infty)^r\exp\left(-\frac{E_a}{R_G T}\right)(C\ -\ C_\infty), \tag{4}$$

The model is subjected to boundary conditions:

$$u=U_1, v=v_w, T=T_w, C=C_w \ \text{ at } y=0,$$
$$u\to U\ \ T\ \to T_\infty, C\ \to\ C_\infty\ \ as\ y\to\infty. \tag{5}$$

The following appropriate variables are applied to the system of flow dimensional equations to obtain dimensionless transformed equations;

$$\left.\begin{aligned} x'=\frac{x}{L}, y'=\frac{y}{\delta}, u'=\frac{u}{U}, v'=\frac{v}{U}\frac{L}{\delta}, p'=\frac{p}{\rho U^2}, U'=\frac{U}{U_0}, \omega'=\frac{4\omega\nu}{v_0^2},\\ V=\frac{U_1}{U_0}, (T-T_\infty)=\left(\frac{E_a}{R_G T_\infty^2}\right)^{-1}\theta(x,y), (C-C_\infty)=(C_w-C_\infty)\theta(x,y)\end{aligned}\right\} \tag{6}$$

where L is scale length, δ is the unknown thickness of the device layer for which $x\ =\ L$, U is the velocity of the flowing liquid along the x-axis parallel to the bounded flow medium layer.

Now, using the defined quantities of equations (6) on the formulated flow boundary equations (1) to (5), the non-dimensional flow system of equations without the prime are obtained as In the limit $R\to\infty$:

$$\frac{\partial u}{\partial x}+\frac{\partial v}{\partial y}=\ 0 \tag{7}$$

$$u\frac{\partial u}{\partial x}+ v\frac{\partial u}{\partial y}=G(x)+\frac{\partial^2 u}{\partial y^2}-H(u-1)\mp Fs(u-1)+Gr(N\theta+\phi) \tag{8}$$

$$u\frac{\partial\theta}{\partial x}+v\frac{\partial\theta}{\partial y}=\frac{\tau}{Pr}\frac{\partial}{\partial y}\left((1+\epsilon\theta)\frac{\partial\theta}{\partial y}\right)+\bar{\beta}\left(\frac{\partial u}{\partial y}\right)^{2}-\bar{\alpha}_{o}[\alpha_{1}(u-1)+\theta] \tag{9}$$

$$u\frac{\partial\phi}{\partial x}+v\frac{\partial\phi}{\partial y}=\frac{1}{Sc}\frac{\partial^{2}\phi}{\partial y^{2}}+\chi\phi-\epsilon\lambda\theta^{r}\exp\left(\frac{\theta}{1+\epsilon\theta}\right)\phi \tag{10}$$

The corresponding boundary conditions becomes:

$$\begin{cases} u'=V,v'=0,\theta(x,0)=1,\phi(x,0)=1, & at\ \ y=0 \\ u'\to 1,\theta(x,y)\to 0,\phi(x,y)\to 1 & as\ y\to\infty \end{cases} \tag{11}$$

The thermo-fluid physical terms are respectively described as follows:

$$\begin{gathered} \frac{\sigma\mu B^{2}(x)L}{kU}=H,\frac{g\beta_{c}(C_{w}-C_{\infty})L}{U^{2}}=Gr,\frac{\beta_{\tau}R_{G}T_{\infty}^{2}L}{\beta_{c}E_{a}(C_{w}-C_{\infty})U^{2}}=N,g\left(\frac{K_{1}}{\nu}\right)\frac{L}{U}|\hat{u}|=Fs,\frac{k}{\rho c_{p}}=Pr, \\ \mu\frac{UL}{\delta^{2}}\frac{E_{a}}{R_{G}T_{\infty}^{2}}=\bar{\beta},\frac{LB^{*}}{U}\left(\frac{\kappa u_{w}(x)}{x\nu}\right)=\bar{\alpha}_{0},\frac{A^{*}(T_{w}-T_{\infty})E_{a}U}{B^{*}bxR_{G}T_{\infty}^{2}}=\alpha_{1},\ k_{r}^{2}\frac{L}{\rho U}\left(\frac{R_{G}T_{\infty}^{2}}{E_{a}}\right)^{r-1}\exp\left(-\frac{1}{\epsilon}\right)=\bar{\lambda} \\ R=\frac{UL}{\upsilon},\frac{R_{G}T_{\infty}}{E_{a}}=\epsilon,D\frac{L}{\rho U}=\frac{1}{Sc},\gamma\frac{L}{\rho U}=\bar{\chi},\qquad\frac{L}{U\delta^{2}T_{\infty}}=\tau,\mu\frac{UL}{\delta^{2}}\frac{E_{a}}{R_{G}T_{\infty}^{2}}=\rho\frac{U^{2}}{\delta^{2}}\frac{1}{\epsilon T_{\infty}}=O \end{gathered} \tag{12}$$

For the flow velocity U parallel to the flat vertical plate, the pressure is independent of y. The condition required at the controlling edge, an indefinite speed gradient $x=y=0$, this depicted that a mathematical singularity solution exist. Meanwhile, an approximate boundary layer implicit is assumed for a drag fluid flow motion at the region along the leading edge. The solution given by the boundary layer approximation is not valid at the main edge, but valid near the point $x=0$. As such, the boundary layer equations (7)-(11) will be reduced single variable independent equations for which the boundary value problem admits a similarity solution.

A one-parameter variable transformations of y,x and ψ for which the dimensionless equations is invariant for ψ. The useful suitable transformation quantities are described as:

$$\begin{gathered} \psi=(2\nu Ux)^{\frac{1}{2}}f(\eta),\ \ v(x,y)=-\frac{\partial\psi}{\partial x}=\sqrt{\frac{U\nu}{2x}}\big(\eta f'(\eta)-f(\eta)\big),\eta=\sqrt{\frac{U}{2\nu x}}y,u=\frac{\partial\psi}{\partial y}, \\ v=-\frac{\partial\psi}{\partial x},\ \ u(x,y)=\frac{\partial\psi}{\partial y}=Uf'(\eta),\quad \eta_{x}=-\frac{1}{2x}\eta,\qquad \eta_{y}=\sqrt{\frac{U}{2\nu x}}. \end{gathered} \tag{13}$$

Using equation (13) on the dimensionless model, equation (7) is identically satisfied. Hence, equations (8) to (11) is transformed to become:

$$f'''(\eta)+f''(\eta)f(\eta)\ -(H\pm Fs)(f'(\eta)-1)+Gr(N\theta+\phi)+G=0 \tag{14}$$

$$\frac{1}{Pr}\Big(\big(1+\epsilon\theta(\eta)\big)\theta'(\eta)\Big)'+f(\eta)\,\theta'(\eta)+\beta(f''(\eta)\,)^{2} -\alpha_{o}[\alpha_{1}(f'(\eta)-1)+\theta(\eta)]=0 \tag{15}$$

$$\frac{1}{Sc}\phi''+\ f(\eta)\phi'+\chi\phi-\lambda\theta^{r}\exp\left(\frac{\theta}{1+\epsilon\theta}\right)\phi=0 \tag{16}$$

$$\begin{gathered} \frac{k}{\mu c_{p}}=\frac{1}{Pr},\qquad\frac{U^{3}\rho L}{\delta^{2}}\frac{E_{a}}{R_{G}T_{\infty}^{2}}=\beta,\frac{2LB^{*}}{U^{2}}\left(\frac{\kappa u_{w}(x)}{\nu}\right)=\alpha_{0} \\ k_{r}^{2}\frac{2xL}{\rho U^{2}}(\epsilon T_{\infty})^{r}\exp\left(-\frac{1}{\epsilon}\right)=\lambda,\frac{DL}{\mu U}=\frac{1}{Sc},\frac{2x\gamma L}{\rho U^{2}}=\chi, \end{gathered}$$

Follow by the transformed boundary conditions

$$\begin{cases} f'(\eta)=V,f(\eta)=0,\phi(\eta)=1,\theta(\eta)=1\text{ at }\eta=0 \\ f'(\eta)\to 1,\qquad\phi(\eta)\to 0,\theta(\eta)\to 0\qquad as\ \eta\to\infty \end{cases} \tag{17}$$

A reduced to two-point boundary layer equation is obtained in the form

$$f'''(\eta)+f''(\eta)f(\eta)=0 \tag{18}$$

Numerically, $f''(0)=0.469599988500248\approx 0.46960$ is obtained and the point solutions are presented in Figure 1.

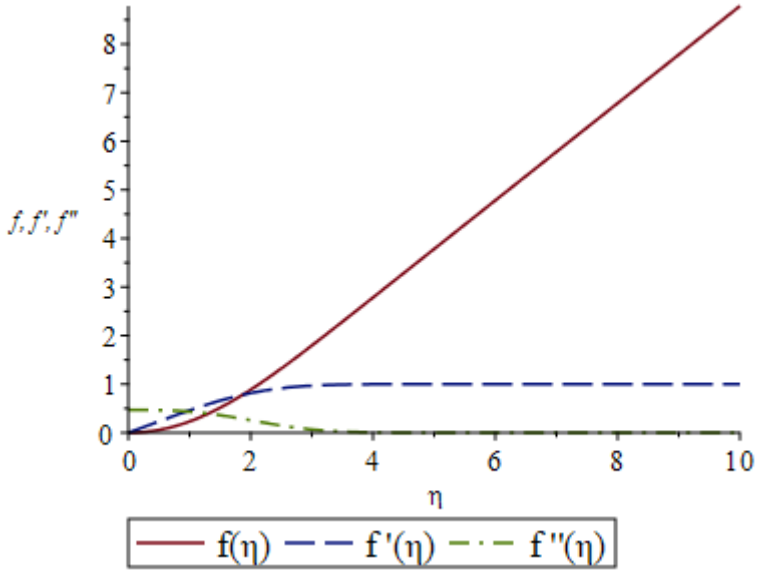

Fig. 1: A one-parameter functions $f(\eta), f'(\eta)$ and $f''(\eta)$.

The range of values at the horizontal axis denoting η is evaluated, while the functions $f(\eta), f'(\eta)$ and $f''(\eta)$ are considered on the vertical axis as presented in Figure 1. The numerical point solutions for the flow field, velocity field and wall velocity gradient are demonstrated in the plot.

3. Numerical Computation Technique

Now, to compute the numerical solution to the problem considered here. The solutions to the system of quasi-linear equations are solved for at the infinite regime $0 < \eta < \eta_\infty$. However, for physical interpretation of results, a finite regime along η −direction is chosen. To ensure that the asymptotic conditions is not affected for an imposed finite domain, the η is taken to be large enough. An independent grid is studied demonstrating that the numerical domain $0 < \eta < \eta_\infty$ can be divided into regular step size interval of 0.02. As such, the number of points reduced in the interval $0 < \eta < \eta_\infty$ with good accuracy. Taking $\eta_\infty = 5$, this is found to be sufficient for the parameter range of values for the computation in this study.

The heat and mass boundary layer governing equations together with the corresponding boundary conditions are given below was numerically solved. The mathematical software Maple 2020 is used run the code for numerical computation of the system of equations (14) – (16) along with initial and boundary conditions (17). The numerical values of the flow governing parameters are chosen to be $\epsilon = N = \lambda = G = 0.1, Pr = 0.71, Sc = 0.6, V = Fs = Bi = H = 0.2, \beta = 0.04,\ Gr = 0.5, \gamma = 0.05, \alpha_0 = 0.02, \alpha_1 = 0.05, r = 1$ based on the existing related theoretical works carried out. The various parameters significantly impact skin friction, Nusselt number, and Sherwood number, which are essential for understanding fluid dynamics, heat transfer, and mass transfer in engineering and scientific applications.

Once we have computed numerically $f(\eta)$ and its derivatives up to second order, we obtain the following table.

Table 1: Effect of α_0, χ, G, H, N and Gr on skin friction, temperature and mass gradient when $\epsilon = \lambda = Pr = 0.71, Sc = 0.6, V = Fs = Bi = 0.2, \beta = 0.04, \alpha_1 = 0.05, r = 1$

α_0	$f''(0)$	$-\phi'(0)$	$-\theta'(0)$	β	$f''(0)$	$-\phi'(0)$	$-\theta'(0)$
α_0 =0	1.1285264	-0.5077929	-0.5139627	β =0.1	1.1283123	-0.5077367	-0.5239178
α_0 =0.2	1.1265668	-0.5072815	-0.6078117	β =2.0	1.1350463	-0.5096857	0.1412231
α_0 =0.4	1.1249422	-0.5068625	-0.6910885	β =4.0	1.1418962	-0.5118670	0.8342117
α_0 =1.0	1.1213691	-0.5059558	-0.8990935	β =8.0	1.1555087	-0.5169522	2.2635433
χ= 0.0	1.0626547	-0.8994555	-0.5172553	V=-0.4	1.4062150	-0.3788426	-0.3788797
χ=0.5	1.0886094	-0.7319737	-0.5198783	V=-0.2	1.3373069	-0.4255151	-0.4307749
χ=1.0	1.2623458	0.1043590	-0.5372888	V=0.2	1.1283123	-0.5077367	-0.5239178
χ=3.0	1.7512308	2.0775658	-0.5768939	V=0.4	0.9923292	-0.5446320	-0.5659391
G=0.0	0.9799411	-0.4876214	-0.5075284	λ = -4.0	1.2594066	0.2375295	-0.5364523
G=0.5	1.6910721	-0.5724704	-0.5720068	λ =-2.0	1.1628269	-0.2957682	-0.5272838
G=1.0	2.3456045	-0.6329471	-0.6082391	λ =2.0	1.0811958	-0.8299286	-0.5192886

G=3.0	4.6745359	-0.7876058	-0.6375864	λ =4.0	1.0218147	-1.3277974	-0.5134954
H=0.0	1.0774817	-0.5066292	-0.5229433	Pr=0.004	1.1470055	-0.5125648	-0.1935291
H=0.4	1.1784640	-0.5089507	-0.5249500	Pr=0.71	1.1283123	-0.5077367	-0.5239178
H=1.2	1.3684251	-0.5140091	-0.5290248	Pr=4.0	1.1160200	-0.5046358	-1.0351951
H=2.0	1.5404663	-0.5186606	-0.5325403	Pr=7.0	1.1128792	-0.5038864	-1.2803677
N=0.0	1.0947979	-0.5050664	-0.5217401	ϵ= 0.01	1.1290445	-0.4992350	-0.5525383
N=0.5	1.2598287	-0.5179152	-0.5320689	ϵ=0.1	1.1283123	-0.5077367	-0.5239178
N=1.0	1.4191753	-0.5296643	-0.5411629	ϵ=0.4	1.1255701	-0.5365213	-0.4529149
N=1.5	1.5737389	-0.5405211	-0.5492400	ϵ=0.8	1.1214260	-0.5753793	-0.3917081
Gr=0.0	0.7287420	-0.4724569	-0.4940437				
Gr=1.0	1.4913757	-0.5355235	-0.5455688				
Gr=3.0	2.7548605	-0.6132785	-0.5935911				
Gr=5.0	3.8569849	-0.6668174	-0.6115227				

From Table 1, we observed that the binary chemical reaction parameter (χ) alters skin friction through changes in fluid viscosity and density, affecting heat and mass transfer rates. The pressure gradient (G) enhances fluid velocity and convective transfer, while the Hartmann number (H) reduces motion and transfer rates due to magnetic field effects. Mass buoyancy (Gr) increases convective transport and gradients, enhancing heat and mass transfer. Suction/injection velocity (V) stabilizes or destabilizes boundary layers, influencing friction and transfer rates. The buoyancy ratio (N) and generative/destructive chemical reaction parameter (λ) adjust transfer rates through buoyancy forces and reaction dynamics.

Further, space heat generation, Arrhenius number, Prandtl number (Pr), and Ohmic heating (β) also play crucial roles. Space heat generation modifies fluid viscosity, affecting friction and transfer rates. Higher Arrhenius numbers and Ohmic heating increase heat generation and transfer rates. The Prandtl number (Pr) impacts velocity and temperature gradients, influencing skin friction and transfer rates. Overall, these parameters interact to shape fluid dynamics, heat, and mass transfer, with applications ranging from metallurgical processes and combustion systems to catalytic reactors and geothermal reservoirs.

4. Results and Discussion

In this study, we have considered those parameters that have significant influence on the flow field. The parameter includes, mass solutal buoyancy (Gr), Ohmic heating (β), viscous dissipation (α_0), Prandtl number (Pr), suction/injection velocity (V), Arrhenius parameter (ϵ), variable temperature parameter (τ), destructive/generative chemical reaction (λ), Hartmann number (Ha) and binary chemical reaction parameter (χ). Here, we discuss the effects and contributions of those parameters on the temperature distribution, concentration and velocity distributions respectively.

4.1 Effects and Contributions of Various Parameters on Temperature Distribution

The sensitivity of the parameters listed above on temperature field is discussed here, considering Fig. 2 – Fig. 9 Solutal buoyancy, often represented by the solutal Grashof number (Gr), measures the buoyancy force induced by concentration differences as shown in Fig. 2. It indicates the relative importance of solutal buoyancy compared to viscous forces in the fluid. Increased solutal buoyancy enhances the convective transport, leading to a more pronounced temperature gradient the result of which is shown as drop in the bulk heat energy. This occurs because the buoyancy-driven flow increases the mixing and transport of heat, for example atmospheric science, solutal buoyancy due to water vapor concentration differences can significantly impact temperature distribution and weather patterns. In Fig. 3, we displayed Ohmic Heating (β), which refers to the internal heating generated due to the electrical resistance of the fluid. Higher values of β result in increased internal heating, raising the fluid temperature. This effect is more pronounced in electrically conductive fluids under the influence of a magnetic field. Example of such could be found in metallurgical processes involving electrolysis.

The effect of viscous dissipation, represented by α_0, accounts for the conversion of mechanical energy into thermal energy due to viscous friction as shown is Fig. 4. Raising this viscous dissipation leads to increased thermal energy generation within the fluid, thereby raising the heat generation. This is crucial in high-speed or high-viscosity flows such as polymer processing, where viscous dissipation can lead to significant heating of the material, affecting its thermal properties and behavior. In Fig. 5, the effect of Prandtl number (Pr) representing the ratio of momentum diffusivity (viscosity) to thermal diffusivity is displayed. It could be observed from the figure that higher Pr values indicate slower thermal diffusion compared to momentum diffusion, resulting in steeper temperature gradients. Conversely, lower Pr values lead to smoother temperature profiles. For example, in gases (low Prandtl number fluids), thermal diffusivity dominates, leading to rapid temperature equalization, whereas in oils (high Prandtl number fluids), temperature gradients are more pronounced. Suction or injection velocity (V) which represents the velocity at which fluid is removed or introduced at a boundary, influencing boundary layer characteristics is displayed in Fig. 6. Suction generally stabilizes the boundary layer, reducing

temperature gradients, while injection enhance mixing and increase temperature gradients. Example is in cooling systems, suction is used to stabilize temperature distribution, whereas injection is used in combustion engines to enhance mixing and combustion efficiency while in Fig 7, the influence of Arrhenius Parameter (ϵ) is depicted. Increasing the values mean that the reaction rate is more sensitive to temperature changes, leading to more pronounced exothermic or endothermic effects, as could be found in chemical reactors, controlling ϵ is crucial for maintaining stable temperature profiles and ensuring reaction efficiency. The effect of The variable thermal conductivity (τ) accounts for temperature-dependent properties of the fluid is shown, increase in the values is shown (Fig. 8) to enhance the temperature. For example, in geothermal reservoirs, the temperature-dependent properties of water significantly impact the heat extraction efficiency and temperature distribution while from Fig.9 the binary chemical reaction parameter (χ) which represents the impact of chemical reactions involving two reactants on the temperature distribution is displayed. Exothermic reactions (positive χ) release heat, decreasing the fluid temperature, while endothermic reactions (negative χ) absorb heat, increasing the temperature. We found such in industrial catalytic converters, where exothermic reactions increase the temperature to the surrounding, enhancing the conversion efficiency of harmful gases to less harmful products.

4.2 Chemical Species Concnetration

The binary chemical reaction parameter (χ) effect which represents the interaction between two chemical species in a fluid flow is displayed in Fig. 10. This parameter is crucial in understanding how the concentration of one species affects the concentration of another a higher value of χ typically indicates a stronger interaction between the chemical species, leading to higher reaction rates. This in turn increase the concentration of reaction products while decreasing the concentration of reactants. While stronger reactions lead to sharper concentration gradients, dictating how species spread within the flow. Example is found in the combustion of hydrogen (H_2) and oxygen (O_2) to form water (H_2O), the binary reaction parameter χ represent the rate at which H_2 and O_2 combine. High values of χ result in rapid formation of H_2O and a quick depletion of H_2 and O_2. Fig. 11 displayed the The generative or destructive chemical reaction parameter λ characterizes whether a chemical reaction is producing (generative) or consuming (destructive) a particular species. When λ is negative, it indicates a generative reaction, leading to an increase in the concentration of the species over time. This can be seen in catalytic reactions where catalysts promote the formation of a product. positive λ signifies a destructive reaction, causing a decrease in species concentration as they are consumed in the reaction. Fig. 12 displayed suction or injection velocity (V) which represents the velocity at which fluid is either removed (suction) or added (injection) to the flow. This parameter is crucial in processes such as cooling, heating, or chemical mixing in industrial applications. Suction ($V > 0$) remove fluid along with its chemical species from the boundary layer. This lower the concentration of reactants/products near the surface, impacting reaction rates and thermal properties. Whereas Injection ($V < 0$) adds fluid and species into the flow, which can increase the concentration of reactants/products at the boundary, enhancing reaction rates and potentially leading to higher temperatures due to exothermic reactions. For example in catalytic converters used in automobiles, injection of additional air (oxygen) can enhance the oxidation of unburned hydrocarbons and carbon monoxide, improving emission quality. On the other hand, suction in certain cooling applications helps in maintaining lower temperatures by removing heated fluid.

4.3 Effects and Contributions on Velocity Distribution

The binary chemical reaction parameter (χ) significantly influences the velocity distribution in fluid flow as shown in Fig. 13. In reactive flows, χ dictates the rate at which chemical species react with one another. A higher χ accelerate reaction rates, altering the fluid's properties, such as density and viscosity, which in turn affect the velocity profile. For instance, in combustion processes, increased χ can lead to more rapid fuel consumption, altering the velocity distribution within the combustion chamber. The pressure gradient (G) is a primary driving force in fluid dynamics, Fig. 14. An increase in the pressure gradient typically results in an increased velocity of the fluid. This principle is applied in pipelines and cardiovascular systems, where higher pressure gradients push the fluid faster. For example, in oil pipelines, maintaining a suitable pressure gradient is essential for efficient transportation of crude oil. The Hartmann number (H) measures the influence of a magnetic field on the fluid flow. In magnetohydrodynamic (MHD) flows, a higher H indicates a stronger magnetic field, which can dampen the fluid motion due to the Lorentz force as displayed in Fig. 15. This damping effect reduces the velocity and creates a more uniform flow profile. In metallurgical processes, where MHD is used to control the flow of molten metals, the Hartmann number is crucial for achieving desired flow characteristics. The mass buoyancy parameter (Gr) Fig. 16, quantifies the effect of buoyant forces due to density differences in the fluid. A higher Gr enhances the buoyant force, which can increase the velocity of the fluid. This effect is prominent in natural convection processes, such as in atmospheric circulation and oceanic currents, where temperature differences lead to buoyancy-driven flows. In Fig. 17, suction ($V > 0$) and injection ($V < 0$) velocities have direct impacts on velocity distribution. Suction tends to decrease the fluid velocity near the boundary due to the addition of fluid, while injection increases the velocity by removal fluid. This is observed in boundary layer control in aerodynamics, where suction is used to delay flow separation and injection is used to reenergize the boundary layer. The buoyancy ratio (N) is the ratio of thermal to solutal buoyancy forces. From Fig. 18, it could be observed that a higher N indicates a dominant thermal buoyancy effect, which increases the velocity distribution and vice versa. In double-diffusive convection, such as in saline water bodies, the buoyancy ratio dictates the relative influence of temperature and concentration gradients on the flow. While in Fig. 19, the generative ($\lambda < 0$) or destructive ($\lambda > 0$) nature of chemical reactions affects the velocity distribution by altering the concentration of reactive species. Generative reactions increase the local density and viscosity, affecting the velocity profile. Destructive reactions have the opposite effect. In catalytic reactors, the parameter λ is essential for optimizing the flow and reaction rates to maximize yield.

5. Conclusion

The dissipative non-slip hydromagnetic flow of Arrhenius kinetics fluid reaction with variable properties is a complex yet critical area of research with substantial practical implications. By building on the existing literature and addressing the identified gaps, this study provide a more accurate and comprehensive understanding of these

phenomena, ultimately contributing to advancements in various engineering and industrial applications. From the discussion in this research, the following observations were made:

- Solutal buoyancy enhances convective transport, affecting weather patterns.
- Ohmic heating raises fluid temperature, significant in metallurgical processes.
- Viscous dissipation influences thermal energy generation, critical in highspeed flows.
- Prandtl number affects temperature gradients, important in gases and oils.
- Suction/injection velocity stabilizes or enhances boundary layer mixing, crucial in cooling systems and combustion engines.
- Arrhenius parameter impacts reaction rates, significant in chemical reactors.
- Variable thermal conductivity affects heat extraction, important in geothermal reservoirs.
- Binary chemical reaction parameter dictates species interaction and concentration, essential in catalytic processes and combustion.
- Generative/destructive reaction parameter modulates species concentration and temperature distribution, crucial in catalytic converters.

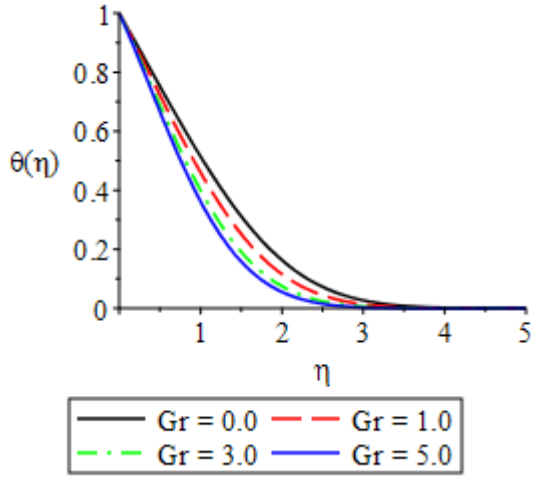

Fig. 2: Effect of (Gr) on heat distribution

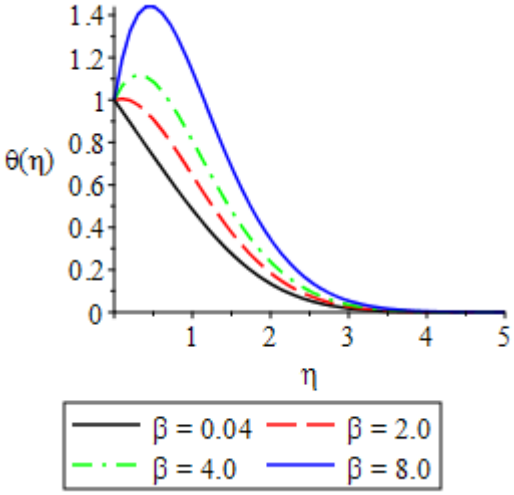

Fig. 3: Temperature profile for various (β)

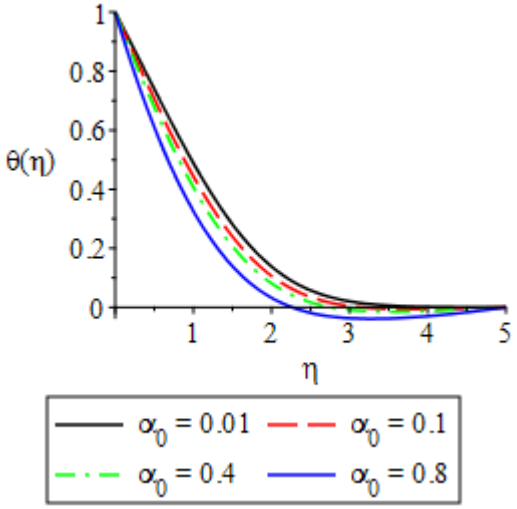

Fig. 4: Reaction of heat profile to rising (α_0)

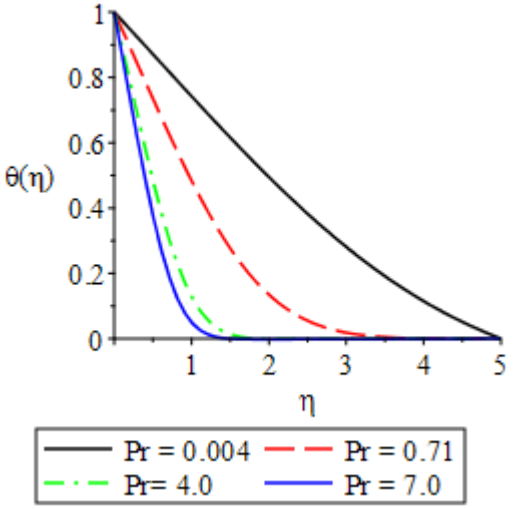

Fig. 5: Rising (Pr) effect on heat profile

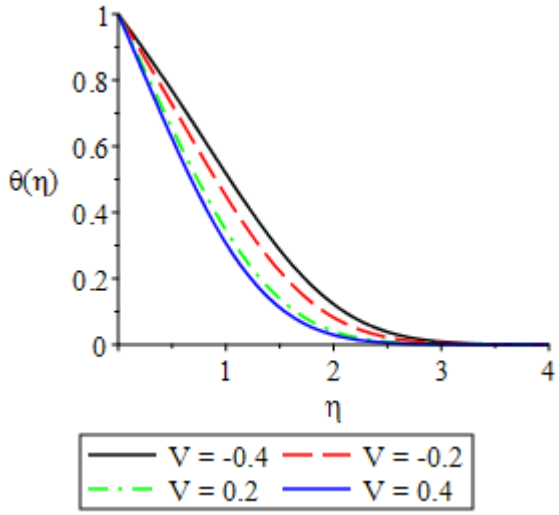

Fig. 6: Impact of suction/injection on heat profile

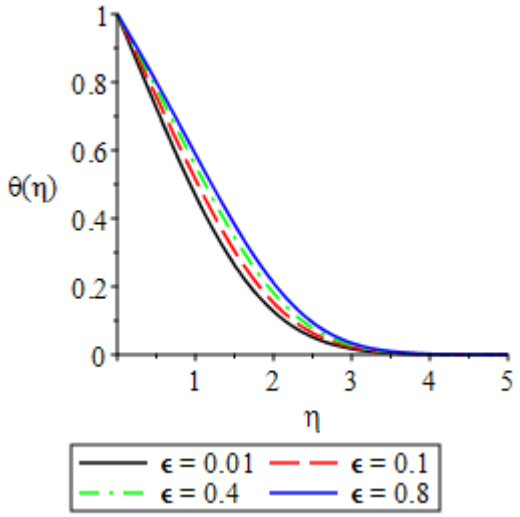

Fig. 7: Impact of (ϵ) on heat distribution

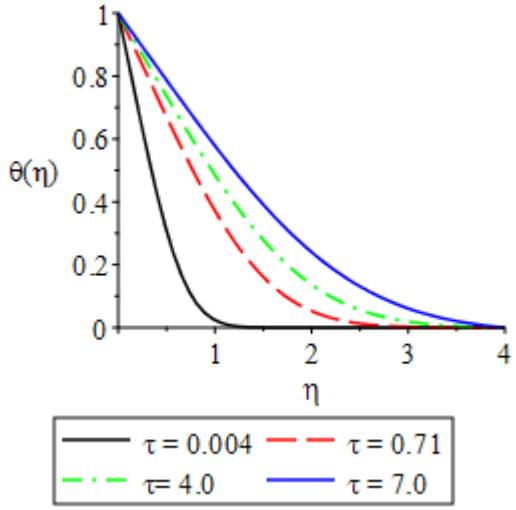

Fig. 8: Influence of variable thermal conductivity on temperature profile

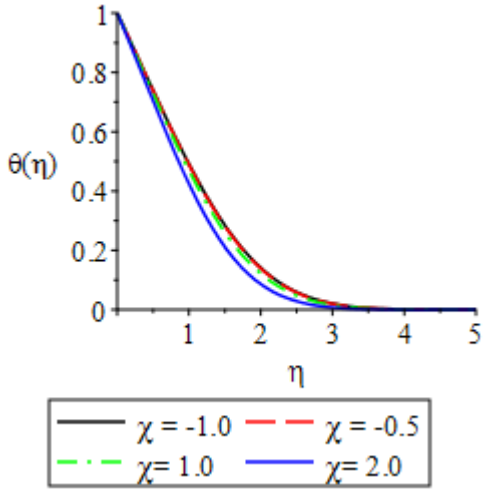

Fig. 9: Effect of Reaction parameter on heat profile

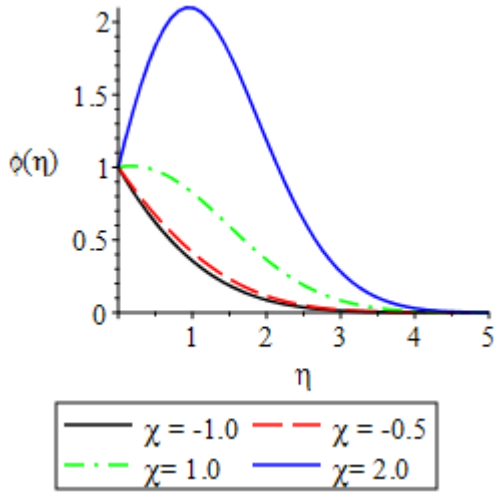

Fig. 10: Mass transfer field for rising (χ)

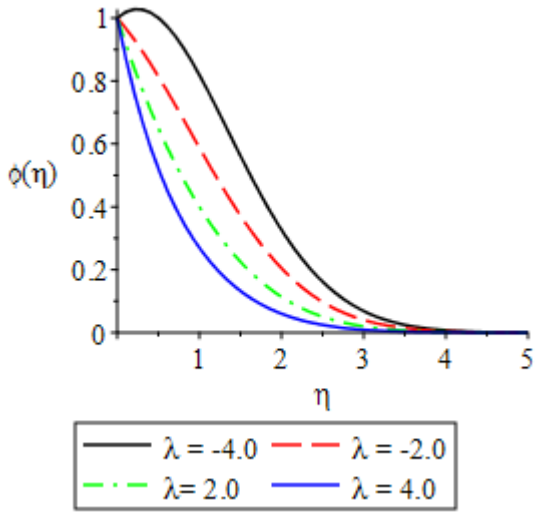

Fig. 11: Mass profile field for various (λ)

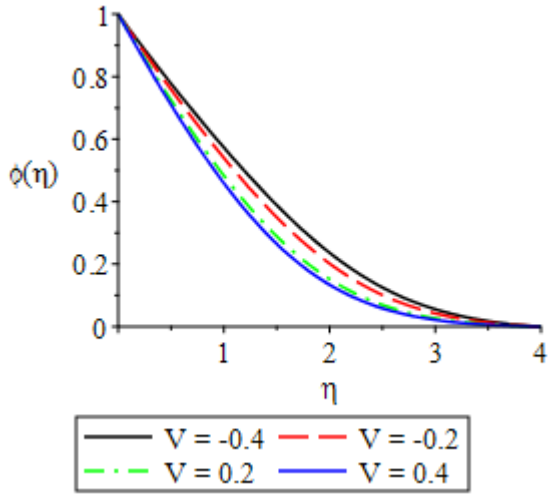

Fig. 12: Effect of Suction/Injection parameter on Concentration profile

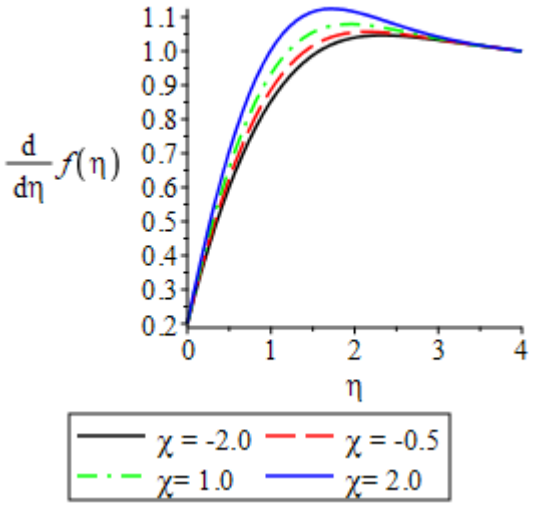

Fig. 13: Effect of χ on velocity distribution

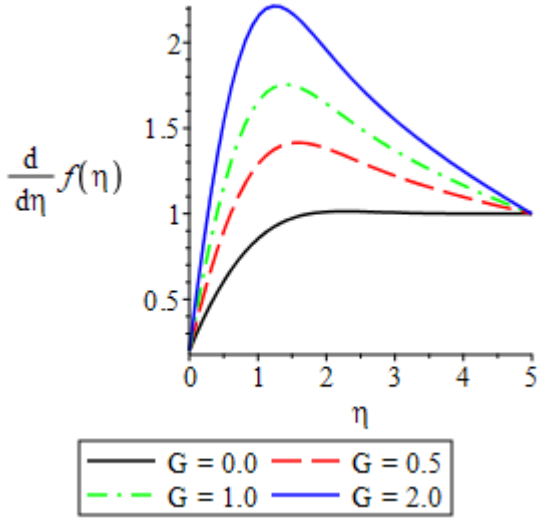

Fig. 14: Velocity field for diverse values of pressure gradient (G)

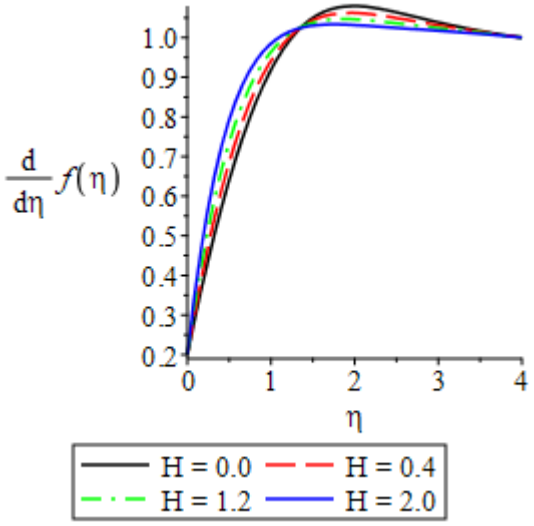

Fig. 15: Velocity field for various values of Hartmann number (H)

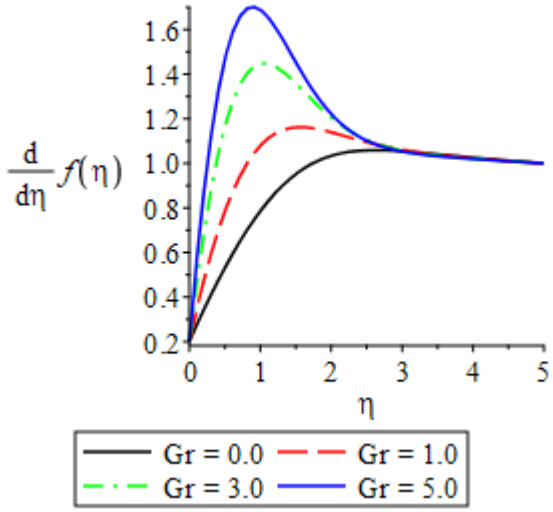

Fig. 16: Impact of mass solutal (Gr) on flow velocity profile

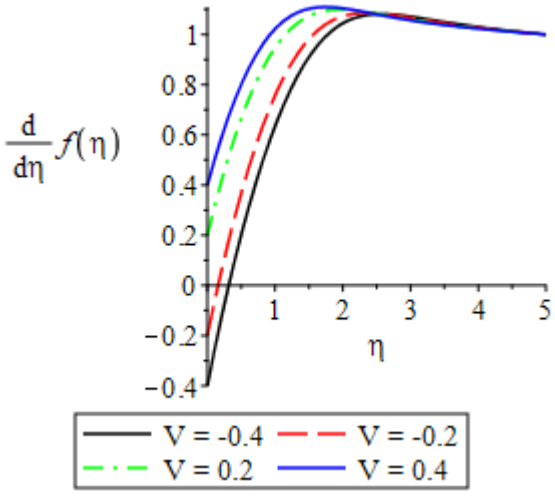

Fig. 17: Velocity Flow rate profile for increasing (V

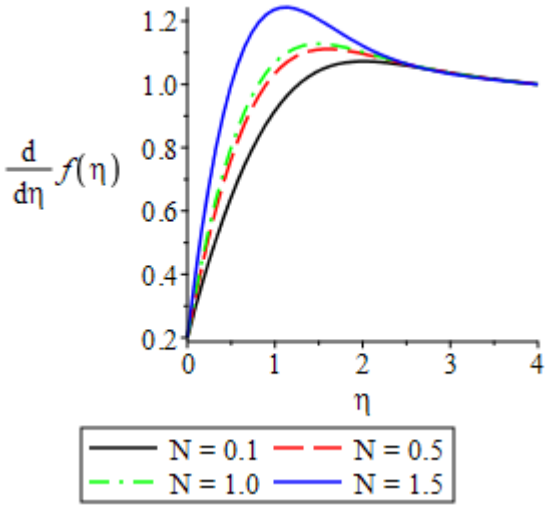

18: Velocity field for different (N)

Fig.

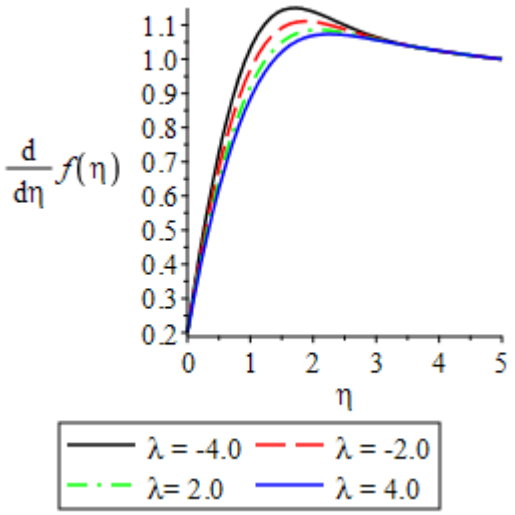

Fig. 19: The (λ) effect on the velocity profile

- Hartmann number influences fluid motion in MHD applications, crucial in metallurgical processes.
- Mass buoyancy enhances fluid velocity, significant in natural convection processes.
- Buoyancy ratio dictates influence of thermal and solutal buoyancy on flow, important in saline water bodies.
- Velocity distribution modulations χ, G, H, Gr, V, N, and λ optimize flow in various applications like combustion, pipelines, and catalytic reactors.
- Parameters such as binary chemical reaction parameter (χ), pressure gradient (G), Hartmann number (H), and mass buoyancy (Gr) significantly influence skin friction by altering fluid viscosity, density, and velocity gradients. Suction/injection velocity (V) and the buoyancy ratio (N) further modulate boundary layer stability and friction.
- The Nusselt number is affected by χ, G, H, Gr, V, λ, space heat generation, Arrhenius number, Prandtl number (Pr), and Ohmic heating (β). These parameters impact the convective and conductive heat transfer rates by modifying temperature gradients and internal heating dynamics.
- Similar to the Nusselt number, the Sherwood number is influenced by χ, G, H, Gr, V, λ, space heat generation, Arrhenius number, Pr, and β. These parameters affect mass transfer rates by altering concentration gradients and species diffusivity.

Acknowledgment:
Authours wish to acknowledge the anonymous reviewers for their valuable suggestions and the effort of the editorial board in maintaining the integrity and quality of this journal.

References

1. Ahmed, J., Shahzad, A., Khan, M., & Ali, R. (2015). A note on convective heat transfer of an MHD Jeffrey fluid over a stretching sheet. *AIP advances*, *5*(11).
2. Bird, R. B., Stewart, W. E., & Lightfoot, E. N. (2002). Transport Phenomena. John Wiley & Sons, Inc. *New York, NY*, *1*.
3. Chamkha, A. J. (2004). Unsteady MHD convective heat and mass transfer past a semi-infinite vertical permeable moving plate with heat absorption. *International journal of engineering science*, *42*(2), 217-230.
4. Cramer, K. R., & Pai, S. I. (1973). Magnetofluid dynamics for engineers and applied physicists.
5. Das, S., & Jana, R. N. (2022). Impact of Variable Viscosity on Boundary-Layer Flows. *International Journal of Thermal Sciences*, 180, 107633.
6. Ghosh, S., Biswas, G., & Mazumder, B. S. (2020). Comprehensive Analysis of MHD Flows with Various Boundary Conditions. *Physics of Fluids*, *32*(11), 114101.
7. Hughes, W. F., & Young, F. J. (1966). The electromagnetodynamics of fluids. *The electromagnetodynamics of fluids.*
8. Kumar, P., Tiwari, A., & Chauhan, D. S. (2021). Effects of Temperature-Dependent Thermal Conductivity in Nanofluids. *Heat and Mass Transfer*, 57, 1591-1603.
9. Okedoye, A. M., & Salawu, S. O. (2019). Unsteady oscillatory MHD boundary layer flow past a moving plate with mass transfer and binary chemical reaction. *SN Applied Sciences*, *1*(12), 1586. https://doi.org/10.1007/542452.019-1463-7
10. Okedoye, A. M., Salawu, S. O., & Asibor, R. E. (2021). A convective MHD double diffusive flow of a binary mixture through an isothermal and porous moving plate with activation energy. *Computational Thermal Sciences: An International Journal*, *13*(5).
11. Olanrewaju, A. M., Salawu, S. O., Olanrewaju, P. O., & Amoo, S. A. (2021). Unsteady radiative

magnetohydromagnetic flow and entropy generation of maxwell nanofluid in a porous medium with arrhenius chemical kinetic. *Cogent Engineering*, *8*(1), 1942639.

12. Metri, P. G. (2017). *Mathematical Analysis of Forced Convective Flow Due to Stretching Sheet and Instabilities of Natural Convective Flow* (Doctoral dissertation, Mälardalen University).
13. Raptis, A., & Perdikis, C. (2020). MHD Flow of a Viscous Fluid over a Stretching Sheet with Thermal Radiation and Variable Viscosity. *International Journal of Numerical Methods for Heat & Fluid Flow*, *30*(2), 697-713.
14. Shercliff, J. A. (1965). Textbook of magnetohydrodynamics.
15. Singh, P. K. (2012). Effects of variable fluid proper ties and viscous dissipation on mixed convection fluid flow past a vertical plate in porous medium. *International Journal of Scientific & Engineering Research*, *3*(7), 1-10.
16. Singh, K., Sharma, A., & Gupta, N. (2023). Influence of Arrhenius Kinetics on Thermal Degradation of Polymers. *Journal of Applied Polymer Science*, *140*(12), 52025.
17. Vishnampet, R., & Anilkumar, P. (2021). Effects of Magnetohydrodynamics on Convective Heat Transfer in Nanofluids. *Journal of Heat Transfer*, *143*(5), 050301.
18. Zhang, H., & Wang, Y. (2022). Impact of Temperature-Dependent Reaction Rates in Catalytic Combustion. *Chemical Engineering Journal*, 430, 132901.
19. Zigta, B. (2018). Effect of thermal radiation, chemical reaction and viscous dissipation on MHD flow. *International Journal of Applied Mechanics and Engineering*, *23*(3), 787-801. Doi: 10.2478/ijame-2018-0043